DOI:10.12119 / j.yhyj.202002004

Extraction Kinetics of Lithium Ions from High Concentration Aqueous Solutions Using Crown Ether and Ionic Liquids

ZHU Wen-bo[1,2,3], JIA Yong-zhong[1,2], SHAO Fei[1,2], ZHANG Quan-you[1,2], YAO Ying[1,2], JING Yan[1,2,*]

(1. *Key Laboratory of Comprehensive and Highly Efficient Utilization of Salt Lake Resources, Qinghai Institute of Salt Lakes, Chinese Academy of Sciences, Xining*, 810008, *China*; 2. *Qinghai Engineering and Technology Research Center of Comprehensive Utilization of Salt Lake Resources, Xining*, 810008, *China*; 3. *University of Chinese Academy of Sciences, Beijing*, 100049 *China*)

Abstract: In this works, the extraction kinetics of lithium from high concentration aqueous solutions using 4'-acetylbenzo-15-crown-5 and 1-butyl-3-methylimidazolium bis[(trifluoromethyl)sulfonyl] imide with constant interfacial area cell are reported. The effects of stirring speed, equilibration time, temperature, interfacial area and the mass transfer resistance zone are studied. The results indicate that the thickness of interface film does not change from 1 600 rpm to 2 000 rpm, the extraction equilibrium time of lithium ions is 40 minutes, the mass-transfer resistance of the extraction process is mainly from organic phase and this extraction process is a mixing-controlled kinetics process that occurs at interfacial area. The extraction kinetic equation of $\nu_{Li,0} = 10^{-3.843 \pm 0.001} \cdot [Li^+]^{0.9071} \cdot [[BMIm]^+]^{0.8328} \cdot [AcB15C5]^{0.8555}$ is obtained by researching the concentration of lithium ions, crown ether, ionic liquids. The extraction mechanism of lithium is deduced by determining the mass-transfer rate step of forming the final complex of lithium ions at the interface, which is consistent with the experimental results.

Key words: Extraction kinetics; Lithium ions; Crown ether; Ionic liquids; Interfacial reaction

CLC number: O642.4 **Document code**: A **Article ID**: 1008 - 858X(2020)02 - 0031 - 13

1 Introduction

Lithium is the world's lightest metal. Lithium has been considered a strategic energy metal that is applied to nuclear fusion reaction [1], aerospace [2], medicine [3], batteries [4] and lubricant [5]. The development of extracting and recovering lithium is particularly important with the increase of lithium demand in recent years. During the past decades, the extraction methods of lithium were reported in literatures, such as adsorption [6], membrane [7], electrophoresis [8], molecular distillation, laser separation and liquid-liquid extraction [9-10]. Among these extraction methods, the liquid-liquid extraction is considered the simple and cost-effective process for lithium extraction.

Owing to high selectivity of crown ether to lithium, crown ether as extractant for extracting lithium have been received universal attention [11]. The commonly reported for extracting lithium with crown ether depended on the 4'-substituted group of benzo-15-crown-5 changing the electronegativity of crown ether ring that influences the ability to bind with

Received date: 2019 - 01 - 02; **Revised date**: 2019 - 01 - 15

First and corresponding author: ZHU Wen-bo. E - mail: jingyan@isl.ac.cn (Y. Jing).

lithium ions[12-13]. In addition, the chemical structures of the Li^+-crown ether complex are simulated by the calculation of molecular mechanics and quantum chemistry [14-15]. In recent years, ionic liquids have been applied in natural organic compounds, or metal ions extraction process, generally with encouraging results [16-18]. Ionic liquid as synergist or solvent doped into the extraction system containing crown ether for extracting lithium ions, which is in favor of improving lithium extraction rate [19]. Therefore, it is necessary to study the novel synergic extraction system consisted of crown ether and ionic liquid for extracting lithium.

If a new extraction system would be used in industrial production, information and data on the equilibrium and kinetics of extraction, and mass-transfer parameters should be given. Several methods to study on kinetics behavior of metal ions extraction system have been developed to now, such as single drop method and constant interfacial area [20-21]. In our works, the extraction kinetics of lithium ions in a novel synergic extraction system consisted of 4'-acetylbenzo-15-crown-5 and [BMIm][NTf_2] were studied by using constant interfacial area cell that is considered to be reliable and simple to operate among the above method mentioned. Various factors affecting the extraction rate of lithium such as the stirring speed, interfacial area, temperature as well as concentrations of Li^+, 4'-acetylbenzo-15-crown-5 and [BMIm][NTf_2] were investigated and analyzed. The kinetics equations were determined by initial concentration method. Then, the extraction mechanism was discussed based on the kinetic result of analysis of lithium extraction from aqueous phase to organic phase.

2 Materials and methods

2.1 Reagents and analytical methods

4'-acetylbenzo-15-crown-5 (abbreviated as AcB15C5) (A. R., >99%) was supplied by Tokyo Chemical Industry Co., Ltd. lithium bis (trifluoromethane) sulfonamide ($LiNTf_2$) was purchased from 3A Chemical Technical Co., Ltd. 1-butyl-3-methylimidazolium bis[(trifluoromethyl) sulfonyl] imide ([BMIm][NTf_2]) was prepared by Lanzhou Institute of Chemical Physics (China). All other reagents used were of analytical purity or highest quality. Ultrapure water was used in experimental process from a Milli-Q purification system. The lithium concentration of aqueous phase was analyzed with inductively coupled atomic-emission spectroscopy (ICP-AES, iCAP6500 DUO, Thermal Electron Corporation). Then the concentration of lithium ions in the organic phase was obtained by the change of lithium ion concentration in the aqueous phase before and after extraction.

2.2 Experimental process

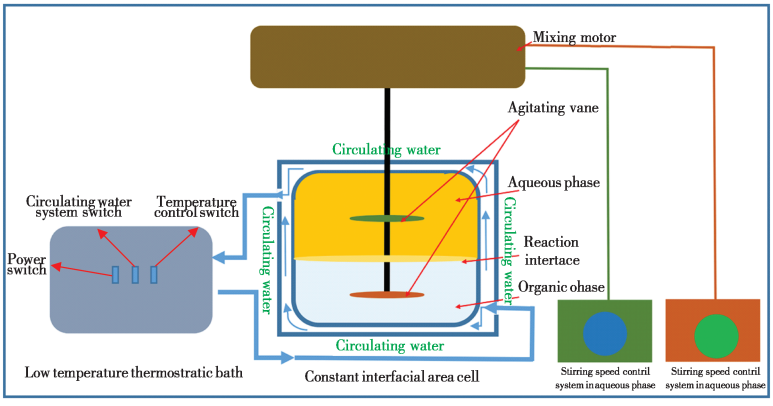

Fig. 1 Diagram of the whole set of devices used in experiments for lithium extraction kinetics

Constant interfacial area cell used in kinetics experiments of lithium extraction is shown as Fig. 1. Constant interfacial area cell with laminar flow had been used as apparatus reported previously, which was proved to be a more reliable technique for kinetics research [22]. In addition, the interface was stable and smooth in the study of kinetics. In our experiments, 25 mL organic phase was placed into the cell, and then the same volume of aqueous phases was carefully poured onto the top of the organic phase and there was no mixing. Before obtaining the sample to be tested, the stirrers in the aqueous and organic phase were rotated at the same speed but in opposite direction for 5 minutes, which resulted in a stable interface between the aqueous phase and the organic phase. In the mass-transfer process, 0.1 mL the solution to be detected and analyzed was removed in aqueous phase every 180 s. The experiments were repeated, and experimental results could be replicated.

2.3 Mathematical relationships of kinetics

It is assumed that the mass-transfer process involves only Li^+ in experiment. According to the method used by Danesi and He [23-24], the following equation would be written:

$$Li^+_{aq} \underset{k_{oa}}{\overset{k_{ao}}{\rightleftharpoons}} Li^+_{org} \tag{1}$$

The mass-transfer rate (ν) through the interface between aqueous phases and organic phases can be obtained as described in equation:

$$v = \frac{dm}{dt} = \frac{V_{aq} d[Li^+]}{S dt} = \frac{V_{org} d[Li^+]_{org}}{S dt} \tag{2}$$

The kinetics equation is confirmed by initial concentration method. The component concentration-times curve is fitted with the function f (t), and the relationship between the mass-transfer rates and times (t) is expressed as follows:

$$v_{Li,0} = f'(t) \tag{3}$$

The reversible reaction is negligible at the beginning of the extraction reaction. The mass transfer rate can be expressed as:

$$v_{Li,0} = k \cdot [Li^+]_0^{n_1} \cdot [[BMIm]^+]_0^{n_2} \cdot [AcB15C5]_0^{n_3} \tag{4}$$

During the extraction experiments, the initial concentration of component B is changed while the initial concentration of other components is kept unchanged. A series of data on the mass-transfer rates are obtained at different initial concentrations of component B. There is a linear relationship between $\ln\nu_0$ and $\ln[B]_0$ since the initial concentrations of other components are the same in each experiment.

$$\ln v_{Li,0} = n \ln[B]_0 + C \tag{5}$$

In this extraction system containing AcB15C5 and $[BMIm][NTf_2]$, $\nu_{Li,0}$ could be written as:

$$\lg(v_{Li,0}) = \lg k + n_1 \cdot \lg[Li^+] + n_2 \cdot \lg[[BMIm]^+] + n_3 \cdot \lg[AcB15C5] \tag{6}$$

The effect of temperature on the extraction rate of Li^+ can be processed by the Arrhenius equation (7) with fixing $LiNTf_2$, $[BMIm][NTf_2]$ and AcB15C5, which can obtain the reaction apparent activation energy (E_a).

$$k = A \cdot e^{-E_a/(RT)} \tag{7}$$

When the concentration of Li^+, $[BMIm]^+$ and AcB15C5 are unchanged, the relationship between $\ln\nu$ and E_a was derived according to Eq. (4), as follows:

$$V_{Li,0} = A_1 \cdot e^{-E_a/(RT)} \tag{8}$$

Taking natural logarithm on each side of Eq. (8), the equation could be translated as follows:

$$\ln v_{Li,0} = -\frac{E_a}{RT} + \ln A_1 \tag{9}$$

Where "aq" and "org" represent respectively the aqueous phase and the organic phase. "k_{oa}" and "k_{ao}" refer to the forward and reverse mass-transfer constants, respectively. "R" is the universal gas constant (8.314 $J \cdot mol^{-1} \cdot K^{-1}$). "$A$" is the pre-exponential factor that is a constant determined only by the nature of a chemical reaction. "T" represented Fahrenheit; "0" represents an initial state. "B" means Li^+ or $[BMIm]^+$ or AcB15C5. "n_1, n_2, n_3" are the reaction order of corresponding components. "n" is the slope that is the same as the reaction order. "A_1 and C" are two constants.

3 Results and discussion

3.1 Effect of the stirring speed

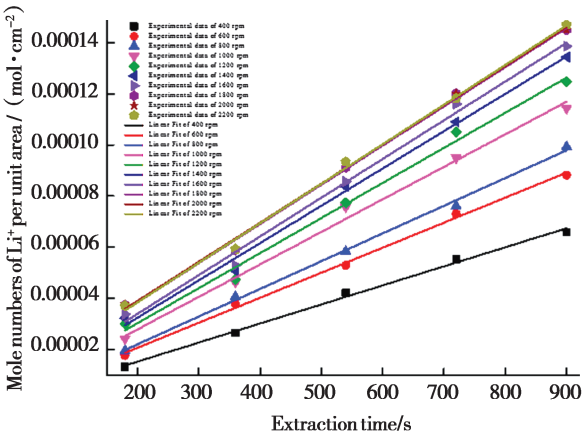

Fig. 2 Fitting linear of mole numbers of Li^+ per unit area vs extraction time. C ($LiNTf_2$) = 1.0 mol·L^{-1}, C (AcB15C5) = 0.2 mol·L^{-1}, C ([BMIm][NTf_2]) = 0.5 mol·L^{-1}, pH = 7.33, S = 9.85 cm^2, T = 298.15 K

Table 1 Variation of equations of fitting linear in Fig. 2 with stirring speed

Equation: f (t) = ν·t + C			
Stirring speed/rpm	Slope /($\times 10^{-8}$)	Intercept /($\times 10^{-7}$)	Adj. R-Square
400	7.456 29	3.096 4	0.994 8
600	9.7941 4	10.355 1	0.996 6
800	10.322 7	3.0454 0	0.996 9
1 000	12.725 6	23.428 3	0.991 4
1 200	13.725 3	27.768 0	0.990 3
1 400	14.601 0	31.902 0	0.993 0
1 600	15.150 8	35.966 2	0.991 3
1 800	15.351 1	76.167 9	0.995 3
2 000	15.317 3	83.324 8	0.994 7
2 200	15.499 1	73.198 9	0.995 9

In solvent extraction kinetics experiments, the effect of stirring speed was investigated firstly that influenced the forward reaction of Li^+ in the two phases. As shown in Fig. 2 and Table 1, we studied the stirring speed from 400 rpm to 2 200 rpm by fitting linear of the Li^+ concentration in the organic phase vs extraction time. The slope of fitting linear was the average mass-transfer rate of Li^+ at a specific stirring speed in Table 1. The relationship between lnν and stirring speed was presented in Fig. 3. Obviously, it was almost a straight line at the stirring speed in range of 400 ~ 1 400 rpm. Results showed that diffusion played a key role in the average mass-transfer rate with the thickness of interface film at slow stirring speed. The average mass-transfer rate was dependent of the stirring speed. After stirring speed increasing, the interface film was going to be thinner and mass transfer was going to be accelerated. Furthermore, the average mass-transfer rate had not changed in range of 1 600 ~ 2 000 rpm in addition to the negligible small variation. This was because stirring speed had a small effect on the average mass-transfer rate, which could be judged preliminarily that the kinetic mechanism of the extraction reaction was a chemical control reaction or a hybrid control mechanism. At this moment, the thickness of interface film no longer changed. All other kinetic experiments were carried out at 1 800 rpm in order to consider only the effect of interface reaction.

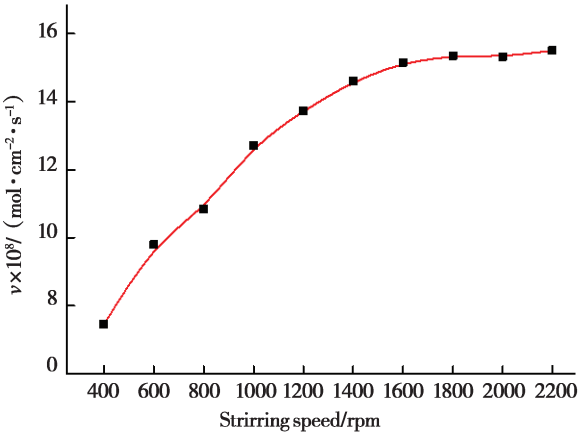

Fig. 3 Effect of stirring speed on the average mass-transfer rate of Li^+ obtained the slope in Fig. 2. C ($LiNTf_2$) = 1.0 mol·L^{-1}, C (AcB15C5) = 0.2 mol·L^{-1}, C ([BMIm][NTf_2]) = 0.5 mol·L^{-1}, pH = 7.33, S = 9.85 cm^2, T = 298.15 K

The influence of the extraction system containing AcB15C5 and [BMIm][NTf_2] on the extraction rate of Li^+ with extraction equilibration time was determined at 293.15 K. The results were shown in

Fig. 4. The extraction process trended to equilibration when extraction time was about 40 minutes. Compared with other extraction systems, the extraction equilibrium time of this system was relatively short. Moreover, the main reason for the result was that the extraction rate of lithium ions in this extraction system was not high, which have been reported in previous literature [10, 19, 25]. In order to ensure mass transfer, all kinetic experiments were far from the equilibrium state of Li^+.

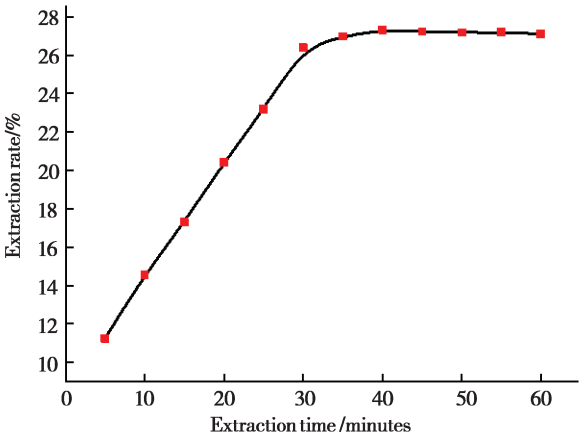

Fig. 4　Equilibration time on extraction at 1 800 rpm. $C(LiNTf_2) = 1.0\ mol \cdot L^{-1}$, C (AcB15C5) = 0.2 $mol \cdot L^{-1}$, C ([BMIm][NTf_2]) = 0.5 $mol \cdot L^{-1}$, pH = 7.33, S = 9.85 cm, T = 293.15 K

3.2　Effect of temperature

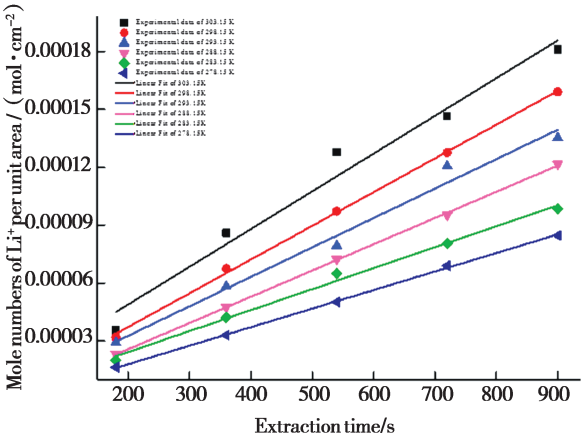

Fig. 5　Fitting linear of mole numbers of Li^+ per unit area *vs* extraction time. C ($LiNTf_2$) = 1.0 $mol \cdot L^{-1}$, C(AcB15C5) = 0.2 $mol \cdot L^{-1}$, C ([BMIm][NTf_2]) = 0.5 $mol \cdot L^{-1}$, pH = 7.33, S = 9.85 cm^2

Table 2　Variation of equations of fitting linear in Fig. 5 with temperature

Equation: $f(t) = \nu \cdot t + C$			
Temperature /K	Slope /($\times 10^{-7}$)	Intercept /($\times 10^{-5}$)	Adj. R-Square
303.15	2.803 16	2.622 24	0.975 6
298.15	2.440 50	1.159 39	0.966 8
293.15	1.529 52	0.204 22	0.962 7
288.15	1.397 49	1.394 93	0.981 5
283.15	1.257 19	1.462 69	0.985 6
278.15	1.031 87	1.567 05	0.993 9

Considering different temperatures have a great influence on the viscosity of solutions and reaction rate, the effect of temperature on the average mass-transfer rate is investigated. The results were presented in Fig. 5 and Table 2. The lithium concentration in the organic phase decreased sharply with increased temperature, which indicated this system was an exothermic reaction to the extraction of lithium ions. In Table 2, the slope of fitting linear was the average mass-transfer rate of Li^+ at a selected temperature. In addition, it can be seen from Fig. 6 that the average mass-transfer rate of Li^+ increased when temperature rose. This phenomenon was because increasing temperature increased the energy of partici-

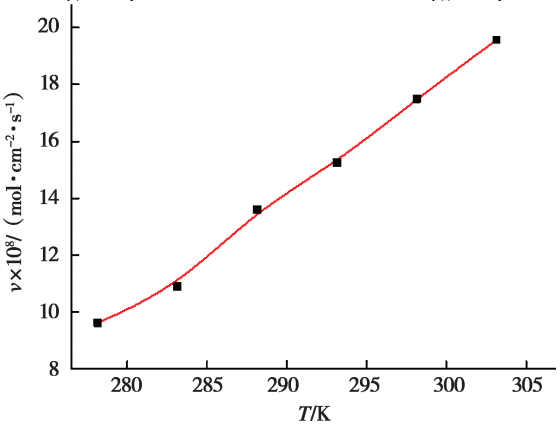

Fig. 6　Effect of temperatures on the average mass-transfer rate of Li^+ obtained the slope in Fig. 5. C ($LiNTf_2$) = 1.0 $mol \cdot L^{-1}$, C (AcB15C5) = 0.2 $mol \cdot L^{-1}$, C ([BMIm][NTf_2]) = 0.5 $mol \cdot L^{-1}$, pH = 7.33, S = 9.85 cm^2

pating, and therefore raised the proportion of activated molecules promoting the average mass-transfer rate of Li^+ in the system.

According to $\ln\nu$ *vs* $10^3/T$, the fitting linear is shown in Fig. 7. From Fig. 7, $\ln\nu$ was proportional to $1/T$, which accords with Arrhenius equation. It is generally believed that temperature has little effect on diffusion control process on extraction but chemical control reaction on extraction is sensitive to temperature. According to Li's and Wang's reports [26-27], the chemical controlled reaction on extraction kinetics keeps the extraction rate of Li^+ under control when the value of the apparent activation energy is more than 40 kJ·mol^{-1}; the diffusion controlled reaction on extraction kinetics keeps the extraction rate of Li^+ under control when the value of E_a is less than 20 kJ·mol^{-1}. In addition, the value of E_a between 20 kJ·mol^{-1} and 40 mol·L^{-1} is considered a mixed controlled regime. In accordance with the slope of the straight line in Fig. 7, the apparent activation energy E_a of the extraction reaction was 20.441 kJ·mol^{-1}, which indicated that the extraction kinetics of this system on extracting Li^+ is a mixed controlled regime within the specified range of 278.15 K ~ 303.15 K.

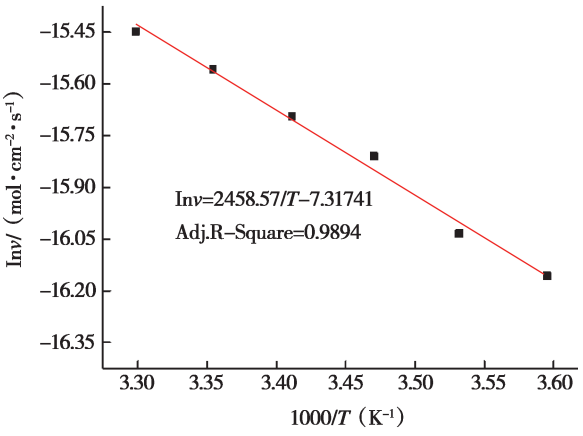

Fig. 7 Fitting straight-line of $\ln\nu$ *vs* 1 000/T. C ($LiNTf_2$) = 1.0 mol·L^{-1}, C (AcB15C5) = 0.2 mol·L^{-1}, C ([BMIm][NTf_2]) = 0.5 mol·L^{-1}, pH = 7.33, S = 9.85 cm^2

3.3 Effect of interfacial area

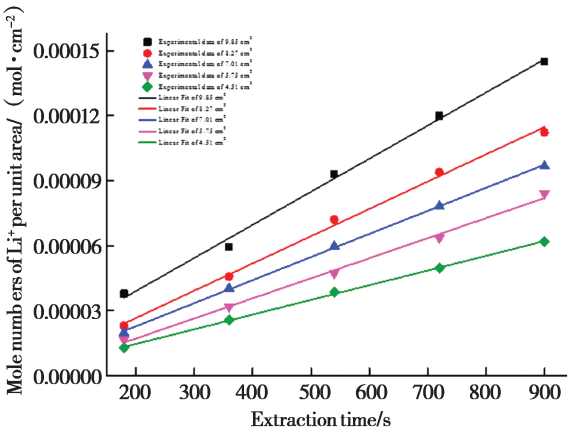

Fig. 8 Fitting linear of mole numbers of Li^+ per unit area extracted into organic phase vs extraction time under different interfacial area. C ($LiNTf_2$) = 1.0 mol·L^{-1}, C (AcB15C5) = 0.2 mol·L^{-1}, C ([BMIm][NTf_2]) = 0.5 mol·L^{-1}, pH = 7.33, T = 298.15 K

Table 3 Variation of equations of fitting linear in Fig. 8 with interfacial area

Equation: $f(t) = \nu \cdot t + C$

Interfacial area /cm^2	Slope /($\times 10^{-8}$)	Intercept /($\times 10^{-6}$)	Adj. R-Square
9.85	15.318 7	8.258 92	0.995 0
8.27	12.623 7	1.182 34	0.995 1
7.01	10.687 1	1.219 70	0.999 3
5.75	9.287 44	−1.621 74	0.994 5
4.51	6.799 71	6.799 71	0.998 8

It is an important content of kinetic research to determine whether the chemical reaction takes place in the bulk phase or at the interface. If the reaction is an interfacial reaction, the mass-transfer rate should be proportional to the interfacial area. The reaction as opposed to the interfacial reaction is independent to the interfacial area. To distinguish between these two types of reactions, the effect of interfacial area on the mass-transfer rate was studied from different interfacial areas in the range of 4.51 cm^2 ~ 9.85 cm^2 as shown in Fig. 8 and Table 3. It is ob-

served that the increase of the interfacial area is beneficial to improve the mass-transfer rate. The relationship between the fitting mass-transfer rate and the interfacial area can be obtained as shown in Fig. 9. The fitting straight line with ν and S is described as $\nu = 1.545\ 07 \times 10^{-8} \cdot S + 7.32451 \times 10^{-11}$. The intercept of fitting line is negligible compared to the data of mass-transfer rates and interfacial areas. Thus, the relationship between the mass-transfer rate and interfacial area is a line passing through the origin. This result suggests that the mass-transfer rate is dependent on the change of interfacial area, and the reaction takes place at interfacial area.

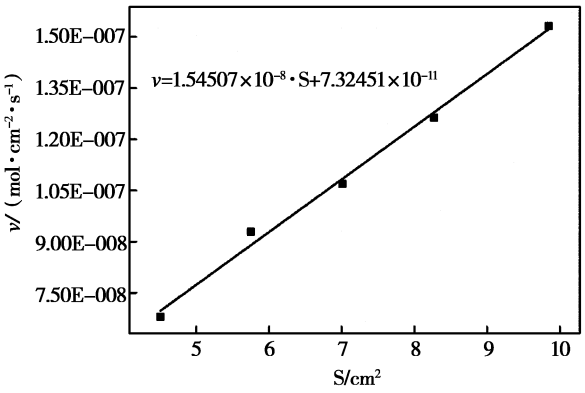

Fig. 9　Effect of interfacial area on the average mass-transfer rate. C ($LiNTf_2$) = 1.0 mol·L^{-1}, C (AcB15C5) = 0.2 mol·L^{-1}, C ([BMIm][NTf_2]) = 0.5 mol·L^{-1}, pH = 7.33, T = 298.15 K

3.4　Determination of the mass transfer resistance zone

To learn more about the mass transfer resistance zone in kinetics experiment, these three situations that stirring is only done in the aqueous phase or stirring is only operated in the organic phase and stirring takes place in the two phases are investigated by the average mass-transfer rate of Li^+ that obtains by the slope of fitting straight-line. The results can be seen from Fig. 10. At the same extraction times, the average mass-transfer rate on lithium ions of only the stirred aqueous phase or the stirred two phases would be greater than the average mass-transfer rate of only the stirred organic phase. This showed that the mass transfer resistance was mainly in organic phase. So, the extraction process occurs mainly on the interface or in the aqueous phase and is almost impossible to occur in organic phase.

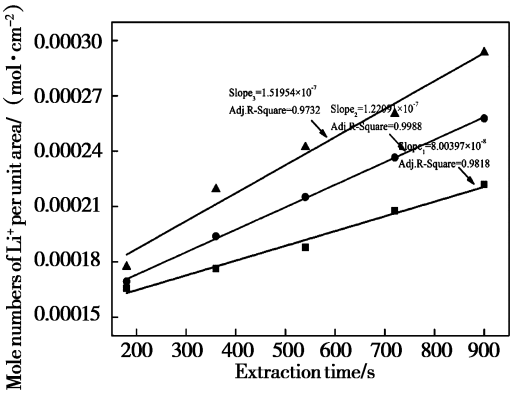

Fig. 10　Effect of different stirring zone on the average mass-transfer rate of Li^+. C ($LiNTf_2$) = 1.0 mol·L^{-1}, C (AcB15C5) = 0.2 mol·L^{-1}, C ([BMIm][NTf_2]) = 0.5 mol·L^{-1}, pH = 7.33, S = 9.85 cm^2, T = 298.15 K

4　Extraction kinetics equation

4.1　Effect of $LiNTf_2$ concentration

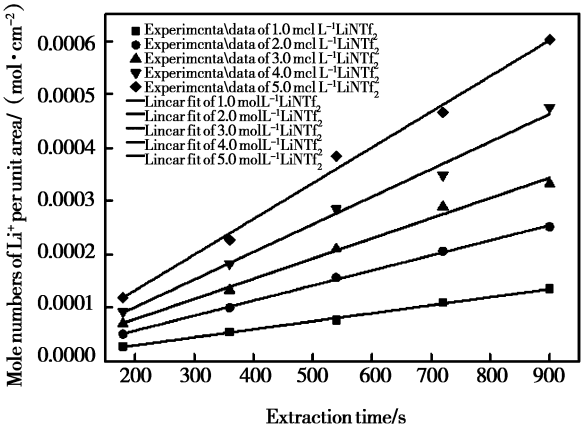

Fig. 11　Fitting linear of mole numbers of Li^+ per unit area extracted into organic phase vs extraction time under different concentrations of $LiNTf_2$ in aqueous phase. C (AcB15C5) = 0.2 mol·L^{-1}, C ([BMIm][NTf_2]) = 0.5 mol·L$^-$, pH = 7.33, S = 9.85 cm^2, T = 298.15 K

Table 4 Variation of equations of fitting linear in Fig. 11 with the concentration of $LiNTf_2$

Equation: $f(t) = \nu \cdot t + C$			
$LiNTf_2$ concentration /(mol·L^{-1})	Slope /($\times 10^{-7}$)	Intercept /($\times 10^{-7}$)	Adj. R-Square
1.0	1.506 49	−7.162 00	0.996 4
2.0	2.822 47	4.631 80	0.998 3
3.0	3.785 25	27.261 4	0.989 9
4.0	5.169 92	−23.754 8	0.989 3
5.0	6.697 12	−15.856 0	0.991 6

From Fig. 11 and Table 4, the average mass-transfer rate is increased when the concentration of Li^+ changes from 1.0 mol·L^{-1} to 5.0 mol·L^{-1}. The result is that the chemical reaction proceeds to the forward reaction with increasing of the initial reactant concentration. In addition, the increasing of the initial reactant concentration enhances the mass-transfer rate of Li^+ by increasing a great number of activated molecules in one-unit volume. As shown in Fig. 12, the lnν has a fine linear relationship with the concentration of Li^+. The fitting slope is determined to be 0.907 1 that is very close to 1. Thus, the extraction reactions are first order reaction on lithium ions based on Eq. (5).

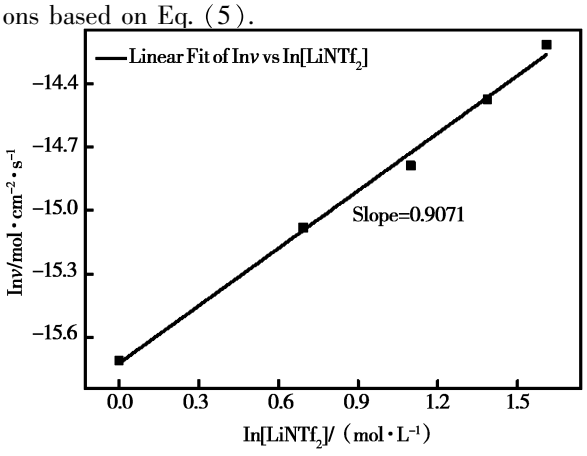

Fig. 12 Effect of the concentration of lithium ions on the average mass-transfer rate. C (AcB15C5) = 0.2 mol·L^{-1}, C ([BMIm][NTf_2]) = 0.5 mol·L^{-1}, pH = 7.33, S = 9.85 cm^2, T = 298.15 K

4.2 Effect of 4'-acetylbenzo-15-crown-5 concentration

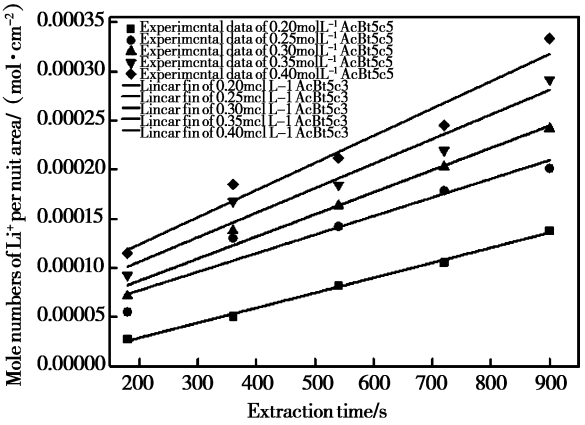

Fig. 13 Fitting linear of mole numbers of Li^+ per unit area extracted into organic phase vs extraction time under different concentrations of AcB15C5. C ($LiNTf_2$) = 1.0 mol·L^{-1}, C ([BMIm][NTf_2]) = 0.5 mol·L^{-1}, pH = 7.33, S = 9.85 cm^2, T = 298.15 K

Table 5 Variation of equations of fitting linear in Fig. 13 with the concentration of AcB15C5

Equation: $f(t) = \nu \cdot t + C$			
AcB15C5 concentration /(mol·L^{-1})	Slope /($\times 10^{-7}$)	Intercept /($\times 10^{-6}$)	Adj. R-Square
0.20	1.530 03	−1.931 35	0.995 5
0.25	1.894 53	39.096 3	0.901 7
0.30	2.255 64	41.667 6	0.972 5
0.35	2.499 71	56.152 6	0.938 7
0.40	2.769 03	68.457 2	0.944 1

It would be seen from Fig. 13 and Table 5 that different concentrations of AcB15C5 in organic phase affect the average mass-transfer rate obviously. In Table 5, the slopes representing the average mass-transfer rate remains increasing with the concentration of AcB15C5 changed from 0.20 mol·L^{-1} to 0.40 mol·L^{-1}. The relationship between lnν and ln [AcB15C5] is studied as shown in Fig. 14. lnν has a fine linear relationship with ln [AcB15C5]. The obtained slope of fitting straight line is determined to

be 0.855 5 that is very close to 1. Thus, the extraction reaction is described as first order reaction on AcB15C5 on the basis of Eq. (5).

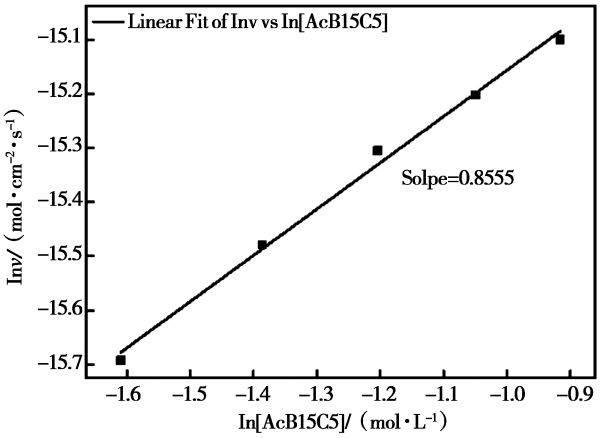

Fig. 14　Effect of the concentration of AcB15C5 on the average mass-transfer rate. C ($LiNTf_2$) = 1.0 mol·L^{-1}, C ([BMIm][NTf_2]) = 0.5 mol·L^{-1}, pH = 7.33, S = 9.85 cm^2, T = 298.15 K

4.3　Effect of [BMIm][NTf_2] concentration

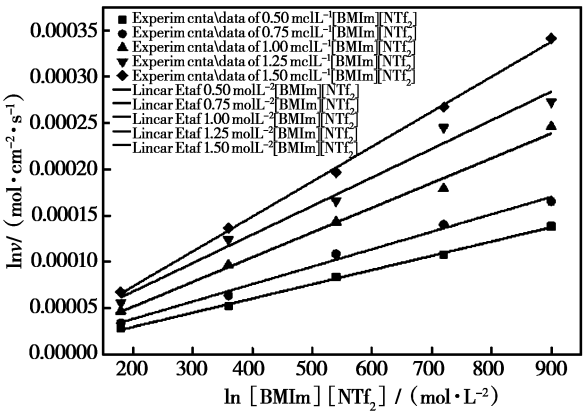

Fig. 15　Fitting linear of mole numbers of Li^+ per unit area extracted into organic phase vs extraction time under different concentrations of [BMIm][NTf_2] in organic phase. C ($LiNTf_2$) = 1.0 mol·L^{-1}, C (AcB15C5) = 0.2 mol·L^{-1}, pH = 7.33, S = 9.85 cm^2, T = 298.15 K

We know from the works of predecessors that the mechanism by which ionic liquids promote the increase of the extractives of metal ions is cation exchange between metal ions and organic cations in ionic liquids [17, 28-30]. It is necessary to investigate the effect of [BMIm][NTf_2] concentration on the average mass-transfer rate in the extraction kinetics experiment. Experiments with [BMIm][NTf_2] concentration changed from 0.5 mol·L^{-1} to 1.5 mol·L^{-1} were conducted. As shown in Fig. 15 and Table 6, [BMIm][NTf_2] concentration has significant effect on the average mass-transfer rate of Li^+. In Table 5, the slopes are the average mass-transfer rates that go up with increase of concentration of [BMIm][NTf_2]. The relationship between lnν and ln [[BMIm][NTf_2]] is studied as shown in Fig. 16. lnν has a fine linear relationship with ln [AcB15C5]. The obtained slope of fitting straight line is determined to be 0.8328 that is very close to 1. Thus, the extraction reaction is described as first order reaction on [BMIm][NTf_2] on the basis of Eq. (5).

Table 6　Variation of equations of fitting linear in Fig. 15 with the concentration of [BMIm][NTf_2]

Equation: f (t) = $k \cdot t$ + C			
[BMIm][NTf_2] concentration /(mol·L^{-1})	Slope /($\times 10^{-7}$)	Intercept /($\times 10^{-6}$)	Adj. R-Square
0.50	1.538 59	1.591 83	0.974 3
0.75	1.862 85	2.427 91	0.991 2
1.00	2.673 41	−2.003 78	0.989 1
1.25	3.492 08	−8.626 58	0.991 1
1.50	3.611 94	3.763 18	0.999 2

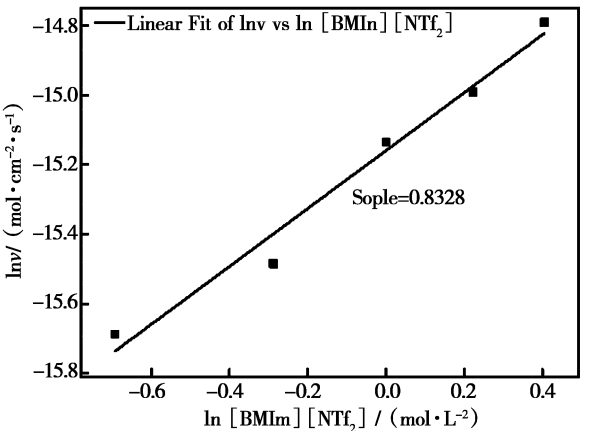

Fig. 16　Effect of the concentration of [BMIm][NTf_2] on the average mass-transfer rate. C ($LiNTf_2$) = 1.0 mol·L^{-1}, C (AcB15C5) = 0.2 mol·L^{-1}, pH = 7.33, S = 9.85 cm^2, T = 298.15 K

4.4 Extraction kinetics equation

The accurate extraction kinetic equation cannot be obtained because k value is unknown. lg k can be obtained by calculating the intercepts of fitting linear in Figs. 11, 13 and 15. Thus, k value is $10^{-3.8437 \pm 0.0001}$ at 298.15 K. Thus, the extraction kinetics equation at 293.15 K can be expressed as:

$$\nu_{Li,0} = 10^{-3.843 \pm 0.001} \cdot [Li^+]^{0.9071} \cdot [[BMIm]^+]^{0.8328} \cdot [AcB15C5]^{0.8555} \quad (10)$$

5 Study on extraction mechanism

According to the above experimental results, the kinetics mechanism of lithium ions with the system containing AcB15C5 and $[BMIm][NTf_2]$ can be described as:

(1) Diffusion balance of extractant and ionic liquid from organic stationary layer to interface:

$$\begin{aligned} AcB15C5_{org} &\underset{k_{-1}}{\overset{k_1}{\rightleftharpoons}} AcB15C5_i \\ [BMIm]^+_{org} &\underset{k_{-2}}{\overset{k_2}{\rightleftharpoons}} [BMIm]^+_i \end{aligned} \quad (11)$$

(2) Diffusion balance of lithium ions from aqueous stationary layer to interface:

$$Li^+_{aq} \underset{k_{-3}}{\overset{k_3}{\rightleftharpoons}} Li^+_i \quad (12)$$

(3) The exchange behavior between lithium ions and cations of ionic liquids at the interface:

$$Li^+_i \underset{k_{-4}}{\overset{k_4}{\rightleftharpoons}} [BMIm]^+_i \quad (13)$$

(4) A chemical reaction between lithium ions and extractant occurred at the interface:

$$Li^+_i + AcB15C5 \underset{k_{-5}}{\overset{k_5}{\rightleftharpoons}} [AcB15C5 \cdot Li]^+_i \quad (14)$$

(5) Diffusion balance of $[BMIm]^+$ from the interface to aqueous stationary layer:

$$[BMIm]^+_i \underset{k_{-6}}{\overset{k_6}{\rightleftharpoons}} [BMIm]^+_{aq} \quad (15)$$

(6) Diffusion balance of the complex $[AcB15C5\cdot]^+$ from the interface to organic stationary layer:

$$[AcB15C5\cdot Li]^+_i \underset{k_{-7}}{\overset{k_7}{\rightleftharpoons}} [AcB15C5\cdot Li]^+_{org} \quad (16)$$

The subscript "i" represents the interface between the aqueous stationary layer and the organic stationary layer. In the above reaction described, the reaction step (1), (2), (5) and (6) are high-speed equilibrium process. And the reaction step (3) and (4) may be the key mass-transfer rate controlling steps in the extraction process of lithium ions. The kinetic equation of Li^+ can be obtained as:

$$v_{Li,0} = k_4 \times k_5 \times C(Li^+)_i \times C([BMIm]^+)_i \times C(AcB15C5)_i \quad (17)$$

In the abovereaction, the following equations can be obtained on basis of the steady-state approximation.

$$C(AcB15C5)_i = \frac{k_1 \times C(AcB15C5)_{aq}}{k_{-1} + k_5 \times C(Li^+)_i} = \frac{k_1(k_{-3} + k_4 + k_5 \times C(AcB15C5)_i) \times C(AcB15C5)_{org}}{k_{-1}(k_{-3} + k_4 + k_5 \times C(AcB15C5)_i) + k_3 \times k_5 \times C(Li^+)_{aq}} \quad (18)$$

$$C(Li^+)_i = \frac{k_3 \times C(Li^+)_{aq}}{k_{-3} + k_4 + k_5 \times C(AcB15C5)_i} \quad (19) \qquad C([BMIm]^+)_i = \frac{k_2 \times C([BMIm]^+)_{aq}}{k_{-2} - k_{-4}} \quad (20)$$

$$v_{Li,0} = \frac{k_1 k_2 k_3 k_5 (k_{-3} + k_4 + k_5 C(AcB15C5)_i) C(Li^+)_{aq} C([BMIm]^+)_{org} C(AcB15C5)_{org}}{(k_{-2} - k_{-4}) \cdot [k_{-3} + k_4 + k_5 C(AcB15C5)_i] \cdot [k_{-1}(k_{-3} + k_4 + k_5 C(AcB15C5)_i) + (k_3 k_5 C(Li^+)_{aq})]} \quad (21)$$

Due to $k_{-3} + k_4 \gg k_5 \cdot C(AcB15C5)_i$, $k_{-1} \cdot (k_{-3} + k_4 + k_5 \cdot C(AcB15C5)_i) \gg k_3 k_5 \cdot C(Li^+)_{aq}$. Thus, Eq. (23) can be expressed as follows:

$$v_{Li,0} = \frac{k_1 k_2 k_3 k_5 \cdot C(Li^+)_{aq} \cdot C(AcB15C5)_{org} \cdot C([BMIm]^+)_{org}}{(k_{-1} + 1) \cdot (k_{-2} - k_{-4}) \cdot (k_{-3} + k_4)} \quad (22)$$

$$k = \frac{k_1 k_2 k_3 k_5}{(k_{-1}+1)\cdot(k_{-2}-k_{-4})\cdot(k_{-3}+k_4)} \tag{23}$$

$$v_{\mathrm{Li},0} = k \cdot C(\mathrm{Li}^+)_{\mathrm{aq}} \cdot C(\mathrm{AcB15C5})_{\mathrm{org}} \cdot C([\mathrm{BMIm}]^+)_{\mathrm{org}} \tag{24}$$

Eq. (25) inferred from the mass-transfer rate determining steps (3) and (4) is consistent with the experimental results.

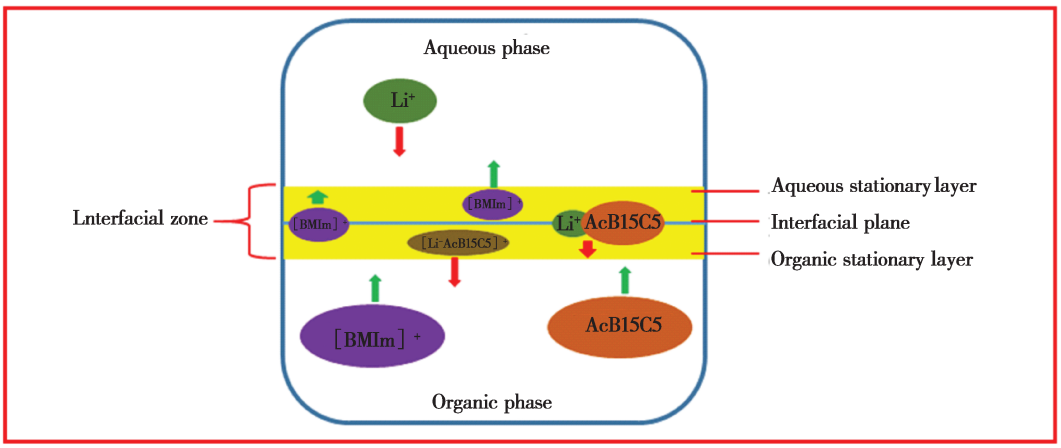

Fig. 17　The illustration of mass-transfer process of lithium ions at interfacial area

6　Conclusions

The extraction kinetics of lithium with 4'-acetylbenzo-15-crown-5 and 1-butyl-3-methylimidazolium bis[(trifluorometyl) sulfonyl] imide dissolved in dichloromethane have been investigated. Various factors including stirring speed, temperature, interfacial area, $LiNTf_2$ concentration, AcB15C5 concentration, $[BMIm][NTf_2]$ concentration were studied respectively through the effect on the average mass-transfer rate of lithium ions. Through the analysis of experimental data of stirring speed, temperature and interfacial area, lithium extraction in the system is controlled by the chemical reaction at the interface between aqueous phase and organic phase. Lithium extraction is first order with changing the concentration of $LiNTf_2$, AcB15C5 and $[BMIm][NTf_2]$. An initial mass-transfer rate equation is inferred to rely on experimental results, which is proposed as $\nu_{Li,0} = 10^{-3.843\pm0.001} \cdot [Li^+]^{0.9071} \cdot [[BMIm]^+]^{0.8328} \cdot [AcB15C5]^{0.8555}$ on lithium extraction by $LiNTf_2$, AcB15C5 and $[BMIm][NTf_2]$. The extraction mechanism of lithium extraction is well deduced by determining the mass-transfer rate step of forming the final complex of lithium ions at the interface, which is consistent with the experimental results.

Acknowledgments

This work was carried out with the support of National Natural Science Foundation of China (U1407117) and the Key Research and Development Program of Qinghai Province (2019-GX-169).

References:

[1] Liu Y K, Liu F, Ye F, Wu F C, Wang Z, Huo X M, Xu J, Chen J. Macrocyclic ligand decorated ordered mesoporous silica with large-pore and short-channel characteristics for effective separation of lithium isotopes: synthesis, adsorptive behavior study and DFT modeling[J]. Dalton T., 2016(45): 16492 – 16504.

[2] Marcoen K, Visser P, Trindade G F, Abel M L, Watts J F, Mol J M C, Terryn H, Hauffman T.. Compositional study of a corrosion protective layer formed by leachable lithium salts in a coating defect on AA2024 – T3 aluminum alloys[J]. Prog. Org. Coat., 2018(119): 65 – 75.

[3] Scott J, Etain J, Bellivier F.. Can an integrated science approach to precision medicine research improve lithium treatment in bipolar disorders? [J]. Bipolar Disord., 2018(9): 1 – 10.

[4] Wang M Y, Huang Y, Zhu Y D, Wu X, Zhang N, Zhang H M.. Binder-free flower-like SnS_2 nanoplates decorated on the gra-

phene as a flexible anode for high-performance lithium-ion batteries[J]. J. Alloy Compd. ,2018(774) :601 – 609.

[5] Wu X H,Zhao Q,Zhao G Q,Liu J M,Wang X B. . Tribological properties of alkylphenyl diphosphates as high-performance antiwear additive in lithium complex grease and polyuria grease for steel/steel contacts at elevated temperature[J]. Ind. Eng. Chem. Res. ,2014(53) :5660 – 5667.

[6] Huang Y,Wang R. . An efficient lithium ion imprinted adsorbent using multi-wall carbon nanotubes as support to recover lithium from water[J]. J. Clean Prod. ,2018(205) :201 – 209.

[7] Shi W H,Liu X Y,Ye C Z,Cao X H,Gao C J,Shen J N. . Efficient lithium extraction by membrane capacitive deionization incorporated with monovalent selective cation exchange membrane [J]. Sep. Purif. Technol. ,2018(210) :885 – 890.

[8] Kamencev M,Yakimova N,Moskvin L,Kuchumova I,Tkach K,Malinina Y,Tungusov O. . Isotopic separation of lithium ions by capillary zone electrophoresis[J]. Electrophoresis,2015(36) : 3014 – 3017.

[9] Shi C L,Jing Y,Xiao J,Wang X Q,Yao Y,Jia Y Z. . Solvent extraction of lithium from aqueous solution using non-fluorinated functionalized ionic liquids as extraction agents[J]. Sep. Purif. Technol. ,2017(172) :473 – 479.

[10] Xiao J,Jia Y Z,Shi C L,Wang X Q,Yao Y,Jing J. . Liquid-liquid extraction separation of lithium isotopes by using room-temperature ionic liquids – chloroform mixed solvent system contained benzo-15-crown-5[J]. J. Mol. Liq. ,2016(223) :1032 – 1038.

[11] Nishizawa K,Ishino S,Watanabe H,Shinagawa M. . Lithium isotope separation by liquid-liquid extraction using benzo-15-crown-5[J]. J. Nucl. Sci. ,1984(21) :694 – 701.

[12] Liu B,Wang S,Jia Y Z,Zhu W B,Zhang Q Y,Wang X Q,Yao Y,Jing Y. . Lithium isotope separation by crown ethers of different nitrogen-containing derivatives in the ionic liquid-anisole system[J]. J. Mol. Liq. ,2019(272) :548 – 553.

[13] Zakurdaeva O A,Asachenko A F,Tophiy M A,Nesterov S V. . Distribution of benzo-substituted crown-ethers between chloroform and water:effects of macrocycle ring size and lithium chloride[J]. J. Radioanal. Nucl. Ch. ,2018(316) :535 – 541.

[14] Torrejos R E C,Nisola G M,Song H S,Lawagon L A,Parohinog K J,Koo S,Han J W,Chung W J. . Design of lithium selective crown ethers:synthesis,extraction and theoretical binding studies[J]. Chem. Eng. J. ,2017(326) :921 – 933.

[15] Cui L,Yang X,Wang J F,He H Y,Guo Y X,Cheng F Q,Zhang S J. . Theoretical prediction of $^{6}Li/^{7}Li$ separation in solvent extraction system using Urey Model[J]. Chem. Eng. J. , 2019(358) :435 – 445.

[16] Sun X L,Zhou W,Gu L,Qiu D,Ren D H,Z. G. Gu,Li Z J. . Liquid-liquid extraction to lithium isotope separation based on room-temperature ionic liquids containing 2,2'-binaphthyldiyl-17-crown-5[J]. J. Nucl. Sci. Technol. ,2015(52) :332 – 341.

[17] Xu J J,Li J Z,Gu Z G,Wang G L,Liu J K. . Green and efficient extraction stratery to lithium isotopes separation with double ionic liquids as the medium and ionic associated agent [J]. J. Radioanal. Nucl. Ch. ,2013(295) :2103 – 2110.

[18] Hoshino T,Terai T. . High-efficiency technology for lithium isotope separation using an ionic-liquid impregnated organic membrane[J]. Fusion Eng. Des. ,2011(86) :2168 – 2171.

[19] Xiao J,Jia Y Z,Shi C L,Wang X Q,Wang S,Yao Y,Jing Y. . Lithium isotopes separation by using benzo-15-crown-5 in eco-friendly extraction system[J]. J. Mol. Liq. ,2017(241) :946 – 951.

[20] Zhang L C,Li L J,Shi D,Peng X W,Song F G,Nie F. . Kinetics and methanism study of lithium extraction from alkaline solution by HFTA and TOPO and stripping process using Lewis Cell technique[J]. Sep. Purie. Technol. ,2010(71) :50 – 55.

[21] Li H F,Li L J,Peng X W,Ji L W,Li W. . Extraction kinetics of lithium from salt lake brine by N,N – bis(2 – ethylhexyl) acetamide using Lewis Cell[J]. Hydrometallurgy,2018(178) :84 – 87.

[22] Huang D F,Zheng H,Li B,Ma G X. . Extraction kinetics of rubidium in brine solutions by 4-tert-butyl-2-(α-methylbenzyl) phenol/sulfonated kerosene using a single drop method[J]. Chem. Phys. Lett. ,2018(713) :105 – 110.

[23] Danesi P R,Chiarizia R. . Mass transfer rate with liquid ion exchangers. The role of interfacial chemical reactions in the extraction kinetics by dinonylnaphthalenesulphonic acid and trilaurylammonium salts[J]. J. Appl. Chem. Biotechnol. ,1978 (28) :581 – 598.

[24] He W W,Liao W P,Wang W W,Li D Q,Niu C J. . Mass transfer kinetics of neodymium (Ⅲ) extraction by calix[4] arene carboxylic acid using a constant interfacial area cell with laminar flow[J]. J. Chem. Technol. Blot. ,2008 (83) :1314 – 1320.

[25] Shi C L,Jia Y Z,Xiao J,Wang X Q,Yao Y,Jing Y. . Lithium isotopes separation by liquid-liquid extraction using ionic liquid system containing dibenzo-14-crown-4[J]. J. Mol. Liq. ,2016(224) :662 – 667.

[26] Javanshir S,Abdolghasemi M,Abolghasem H,Darban A K. . Kinetics of Au (Ⅲ) extraction by DBC from hydrochloric solution using Lewis Cell[J]. Int. J. Miner. Process,2011(98) :42 – 47.

[27] Wu D B,Wang X L,Li D Q. . Extraction kinetics of Sc (Ⅲ), Y (Ⅲ),La (Ⅲ) and Gd (Ⅲ) from chloride medium by Cyanex 302 in heptane using the constant interfacial cell with laminar flow[J]. Chem. Eng. Process,2017(46) :17 – 24.

[28] Dietz M L,Dzielawa J A,Laszak I,Young B A,Jensen M P. . Influence of solvent structural variations on the mechanism of facilitated ion transfer mechanism of facilitated ion transfer into room-temperature ionic liquids[J]. Green Chem. ,2003(5) : 682 – 685.

[29] Dietz M L,Stepinski D C. . Anion concentration-dependent par-

titioning mechanism in the extraction of uranium into room-temperature ionic liquids[J]. Talanta,2008(75):598 - 603.
[30] Garvey S L,Dietz M L. . Ionic liquid anion effects in the extraction of metal ions by macrocyclic polyethers[J]. Sep. Purif. Technol. ,2014(123):145 - 152.

冠醚/离子液体体系对锂离子萃取动力学的研究

朱文波[1,2,3],贾永忠[1,2],邵　斐[1,2],张全有[1,2],姚　颖[1,2],景　燕[1,2,*]
(1. 中国科学院青海盐湖研究所,中国科学院盐湖资源综合高效利用重点实验室,青海 西宁　810008;
2. 青海盐湖资源综合利用工程技术研究中心,青海 西宁　810008;
3. 中国科学院大学,北京　100049)

摘　要:本文通过恒界面池法研究了以 4'—乙酰基苯并—15—冠—5 作为萃取剂和 1—丁基—3—甲基咪唑双[(三氟甲基)磺酰基]酰亚胺作为协萃剂的萃取体系从高浓度水溶液中提取锂的动力学。研究了搅拌速度、平衡时间、温度、界面面积和传质阻力区对锂离子传质速率的影响。结果表明,界面膜的厚度在 1 600 rpm ~ 2 000 rpm 转速范围内是逐渐变薄的,并且在 1 800 rmp ~ 2 000 rmp 转速范围内是没有变化的,说明锂离子传质速率 1 800 rmp ~ 2 000 rmp 转速范围内是不变的;在锂离子的萃取平衡时间为 40 min;萃取过程的传质阻力主要来自有机相;该萃取过程是混合控制的动力学过程;在两相界面上发生的萃取反应。通过研究锂离子、冠醚离子液体的浓度,锂离子的动力学方程可表达为:$\nu_{Li,0} = 10^{-3.843 \pm 0.001} \cdot [Li^+]^{0.907\,1} \cdot [[BMIm]^+]^{0.832\,8} \cdot [AcB15C5]^{0.855\,5}$。通过两相界面处形成锂离子最终配合物的传质速率步骤推导出锂的提取机理,这与实验结果一致。

关键词:萃取动力学;锂离子;冠醚;离子液体;界面反应

封面图片:翡翠湖

翡翠湖是大柴旦湖的一角,位于青海省西北部,柴达木盆地北缘。因其如翡翠一般纯澈清灵的湖水而成为网红旅游打卡地,它位于白雪皑皑的祁连山达肯达坂下,常年的冰雪融水滋润和强烈的蒸发环境下,形成独特的雪山—湿地—盐湖自然景观。实际上翡翠湖是历经多年的盐湖开采而形成的采坑,由于所含的矿物质浓度的不同,而形成颜色多彩的景象,特别是风平浪静的时刻,蓝色和绿色宝镜般的小湖散布在四周,倒映着蓝天白云和红旗雪峰,宛如仙境。翡翠湖水矿化度在 340 ~ 380 克升,矿物质组分以氯化钠、硫酸镁、氯化钾以及硼酸盐为主,具有较高的工业开采价值。

(中国科学院青海盐湖研究所　李建森)